Current Chemistry Letters 13 (2024) 187–198

Contents lists available at GrowingScience

Current Chemistry Letters

homepage: www.GrowingScience.com

Predictive study, using density functional theory and time dependent functional theory, on the structure-property quantification of methylene blue and methyl red dyes for the application in organic solar cells

Latifa Amini[a], El Hassan El Karni[a], Mustapha Oubenali[a*], Hayat El Ouafy[a], Mohamed Mbarki[a] and Brahim El Ouadi[b]

[a]*Laboratory of Engineering in Chemistry and Physics of Matter, Faculty of Science and Technologies, Sultan Moulay Slimane University, BP 523, Beni-Mellal, Morocco*
[b]*ENSAM Rabat, Morocco*

C H R O N I C L E

Article history:
Received December 25, 2022
Received in revised form
June 3, 2023
Accepted July 7, 2023
Available online
July 7, 2023

Keywords:
Methylene Blue
Methyl Red
UV-Visible spectrum
DFT
OPV

A B S T R A C T

In this work, two organic materials as dyes, namely, methylene blue (MB) and methyl red (MR), have been proposed to play the role of the electron donor in organic photovoltaic (OPV) cells. We use the PCBM as a well-known electron acceptor. The density functional theory (DFT) method has been used to determine the electrostatic potential and the frontier molecular orbitals (FMO), of the methylene blue (MB) and the methyl red (MR) compounds. Nonlinear optical (NLO) descriptors have been determined for the two compounds. The potential energy surface analysis has been performed by the DFT method using the exchange and correlation of Becke, Lee, Yang, and Parr Gradient Corrected Functional (B3LYP) with the standard 6-31G(d) base. We have performed another theoretical study using quantum time-dependent density functional theory (TD-DFT) on both MB and MR as organic dyes to determine their UV-Vis spectra. The results of the energy gap, chemical hardness, dipole moment, and hyperpolarizability show that MB may be chemically more reactive Than MR. The present work has proposed a bilayer organic photovoltaic (OPV) cell to contribute to the valorization of the two dyes as solar materials. The developed photovoltaic cell project has used electrical and energetic parameters that can describe the OPV cell based on ([MB or MR]: PCBM). Open-circuit voltage (Voc), excitation energy, and oscillator strength have been theoretically determined. The results of the present work showed a remarkably high open circuit voltage, especially in the case of methyl red (1.55 V) more than in the case of the methylene blue (0.84 V) so that both of the two dyes can be a good candidate for organic solar cells.

1. Introduction

Solar energy is the safest, most reliable, and cleanest natural energy by far. As a renewable energy it is obtained from the use of electromagnetic radiation from the Sun. Man has used the solar radiation that reaches the Earth since ancient times, thanks to different technologies that have evolved, and Photovoltaic (PV) power generation is one of the most essential ways of utilizing solar energy in the world. In the face of the crisis on global energy and the environment today, PV power generation has apparent advantages in resource sustainability and environmental friendliness.[1] The Photovoltaic industry has been explosively developed based on the combination of semiconductor technology and new energy requirements, and has been taken as an important development direction of China's strategic emerging industries.[2] Silicon solar panels are currently the most popular; but this technology presents a very high cost. Organic photovoltaic materials can be an alternative solution, since the manufacturing of these compounds are much less expensive and does not require a higher initial investment.[3,4] In addition, organic devices can be elaborated on flexible or semi-transparent substrates and can

* Corresponding author.
E-mail address m.oubenali@usms.ma (M. Oubenali)

doi: 10.5267/j.ccl.2023.7.002

benefit from new applications, such as solar textiles that wrap for easy transport, solar tinted windows.[5,6] Scharber and al. have proposed a semi-empirical model in 2006 to explain the operation of the organic devices and provide an efficiency maximum of 11% based on this model.[7] The so-called *ab-initio* calculations methods, that have been used in this model to solve Schrödinger equation, are not based on experimental data. In fact, an interesting technique to resolve the Schrödinger equation is the density functional theory.[8]

Organic semiconductors have become very interesting to both theoreticians and experimentalists in recent years, thanks to their excellent optical and electronic properties.[9] These materials can be used for producing such diverse devices as photovoltaic cells, field effect transistors, and light emitting diodes.[10,11–13] Most research of new conjugated molecules with specific applications has been one of the attractive topics in the fields of physical and chemical materials.[14–16] A necessary understanding of the relationship between structure and properties of these materials is desired to exploit their properties for photovoltaic cells. It is well known that organic photovoltaic (OPV) cells have recently provided considerable attention, thanks to the inexpensive manufacturing and wide variety of functionalities of organic materials.[17–19] Their characteristics of implementation could ensure new applications such as to allow the development of mobile technologies like those applied in the cases of telephones and computers. The performance of organic cells is dependent essentially on the active layer made of organic materials between the electrodes. Over the past two decades, two types of organic solar cells have been remarkably studied: The monolayer OPVs that present a single layer and bilayers ones that are constituted by a stack containing two organic layers. The conduction of these materials is ensured thanks to the presence of the system of π electrons as delocalized electrons over the compound. This endows original properties to the conjugated systems compared to the saturated ones.

The main objective of this work is to carry out a quantum study of methylene blue (MB) and methyl red (MR) dyes (**Fig. 1**) in the fields of physical and chemical materials in order to exploit their properties for photovoltaic cells. Methylene blue is a phenothiazine-related heterocyclic aromatic compound ($C_{16}H_{18}N_3SCl$). It is a solid, odorless, dark green powder at room temperature that yields a blue solution when it is dissolved in water.[20,21] Methylene blue is used in a wide variety of settings and for many purposes; for example, as a redox indicator or as a dye/stain.[22,23] Is a selective inhibitor of guanylate cyclase, a second messenger involved in nitric oxide-mediated vasodilation.[24,25] Methyl red is a color indicator of pH and is an indicator of acid-base titrations. The acid form of methyl red exists in zwitterionic (protonated form) as HMR, whereas in its basic form. It is in the anionic form (deprotonated acid) as MR.[26] According to the work of Jasiński et al. we observed that the structures of MB and MR can be considered as zwitterions that would present a lengthening of multiple bonds and a shortening of the delocalization of electrons along the so-called push-pull system. [27]

In this work, we are interested in studying the structural properties of methylene blue and methylene red. We have used the method of quantum density functional theory (DFT) to calculate: several descriptors such as: optimizing geometries, energies and densities of the HOMO- and LUMO frontier molecular orbitals, electronic chemical potential, electronegativity, chemical hardness, global softness, global electrophilic index, global nucleophilic index, nonlinear magnetic optical properties and potential molecular electrostatics. In order to be able to verify the capacity of the MB and MR molecules to allow a photovoltaic application. By determining these quantum descriptors, we found that the MB dye has good conductivity and is an excellent semiconductor. The current results of this current work have led us to a candidate molecule MB for the application of organic solar cells as a means of utilizing green energy.[28,29] So, the OPV cell model that we present in the present work is based on the conduction by electrons and holes, as well as the presence of a HOMO band, a LUMO band, a forbidden band.[18] In the present work we propose, using calculations by DFT and TD-DFT methods, to determine performances of MB and MR as materials for PVO cell. The technique considers that Donor/Acceptor heterojunction cell contains a (MB or MR) molecule which constitutes an organic donor semiconductor and the [6,6]-phenyl-C(61)-butyric acid methyl ester (PCBM) which constitutes an acceptor organic semiconductor.

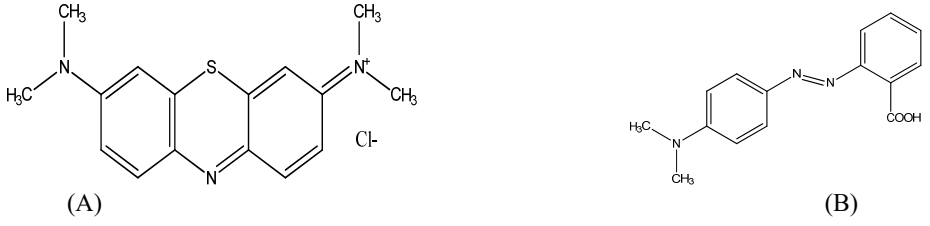

Fig. 1. Expanded chemical formulas: (A) Methylene blue and (B) Methyl red

2. Constitution and principles of proposed organic photovoltaic cells

2.1. Structure of the proposed organic photovoltaic cells

The structure that the present work proposes as an organic photovoltaic (OPV) bilayer cell is shown in **Fig. 2**. This OPV cell is constituted of a metallic cathode (Al), an active bilayer, an anode that is made of ITO (Indium-doped Tin Oxide) and

glass substrate. In fact, being highlighted by the results of previous work[30], we suggest that this bilayer consists of two organic semiconductors of different types. The first layer is a "D" electron donor and the second one is an "A" electron acceptor. One can observe that such a cell develops a D/A interface which can separate charges. So, the donor and acceptor are chosen so that the HOMO and LUMO levels ensure the transfer and transport of the charges.[31] In fact, the donor layer (D) is constituted from a dye as conjugated system (methylene blue (MB) or methylene red (MR)) and the A layer is from a large acceptor molecule (PCBM). This choice of molecule or compound is made to have difference in energies between the LUMO of the donor and acceptor leading to a performance. The electrodes that we suggest are chosen so that we can obtain ohmic contacts with the organic films. So, the cathode should be in contact with the electron acceptor while the anode is so with the electron donor and the cathode with the electron acceptor. One can use Indium-doped tin oxide (ITO) as a semi-transparent electrode, thanks to its high transmittance on the one hand and its ohmic contact with hole-carrying materials, on the other hand. Finally, we note that to ensure an ohmic contact with n-type materials the suggested rear electrode is made of metals such as Al, Ag or Mg-Ag alloys.

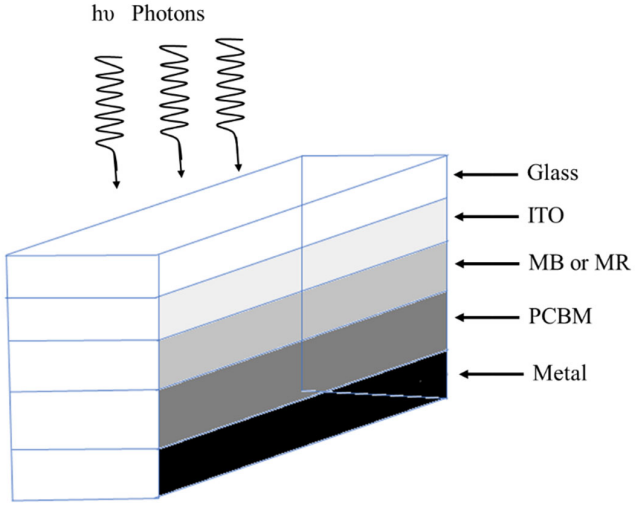

Fig. 2. Proposed structure of the MB- or MR OPV cell.

2.2. Principles of operation of an organic photovoltaic (OPV) cell

We describe the general operating principle of a D/A OPV bilayer cell by the three steps that are photon absorption, exciton diffusion and charges separation. When light passes through the active layer of the photovoltaic cell, a photon is absorbed by this layer so that an electron – hole pair (exciton) is produced. It is known that such an exciton corresponds to the electron transition from the HOMO energy level of a molecule to its LUMO one. In fact, such a transition is carried out thanks to the contribution of energy of the absorbed photon. The exciton diffuses towards the interface (electron donor/electron acceptor) between the organic materials. If the excitons are generated at a 5 to 20 nm distance that is less than the so-called the exciton diffusion length, they can diffuse to the interface, otherwise they recombine.[32-34] The dissociation of the excitons, when they join the D/A junction, takes place at the interface between the two materials. So, a pair of polarons is then obtained: appositive charge (hole) in the electron donor and a charge negative (electron) in the acceptor. [35] The determining factor for dissociation is the difference in energy levels between the LUMO level of the electron donor and the LUMO one of the electron acceptors. If the difference between these two levels is not at least 0.30 eV, the dissociation is likely. However, beyond this value, the charge transfer takes place normally so that the exciton will be dissociated.

2.3. Equivalent electric diagram of the proposed OPV cell

If we consider the simple case of an ideal cell with a donor-acceptor OPV subjected to a light flux, it functions as a current generator. Its equivalent diagram **(Fig. 3)** is represented by an ideal diode connected in parallel with a current source. Rs is a series resistance related to volume resistivity and impedance of electrodes and materials. It is known that the slope of the I(V) curve at the point V_{oc} represents the inverse of the series resistance ($1/R_s$). The R_{sh} term corresponds to a parallel resistance related to edge effects and volume recombination. The slope of the I(V) curve at the I_{cc} point represents the inverse of the shunt resistance ($1/R_{sh}$). So, in order to minimize losses, decrease Rs and increase Rs, the ideal case is represented by R_{sh} equal to infinity and R_s equal to zero.[36] So the equivalent electric circuit is shown in **Fig. 3**. The single diode model has been proposed by B. Mazhari to model organic photovoltaic cells.[37] The equivalent electric circuit of the model that we propose for the present photovoltaic cell is shown in **Fig. 3**. This model contains a photo-current generator

I_{ph}, a diode that represents the Shockley diffusion current (I_d), with its saturation current I_0 and its ideality factor n, two parasitic resistances: the series resistance R_s and the parallel resistance R_{sh}.

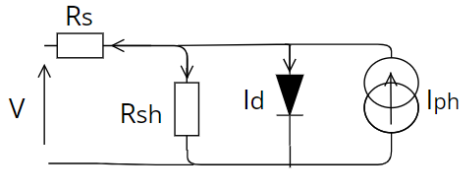

Fig. 3. Equivalent circuit scheme for the proposed organic photovoltaic cell, with: I_{ph}: photo-current, I_d: Shockley diffusion current, R_s: series resistance, R_{sh}: series resistance and V: voltage.

3. Computational methods

All the calculations in this study have been performed thanks to the Gaussian 09 software. The optimized geometry of methylene blue and methylene red has been calculated using the B3LYP/6-31G(d) base. So, the lengths of the chemical bonds and their connection angles have been fully optimized by the DFT method. The following quantum chemical indices have been taken into account: the energy of the highest occupied molecular orbit (E_{HOMO}), the energy of the lowest unoccupied molecular orbit (E_{LUMO}), the energy band gap ($\Delta E = E_{HOMO}-E_{LUMO}$), electron affinity (A) and ionization potential (I). Moreover, the UV spectrum has been studied using the time-dependent density functional theory (TD-DFT) method.

4. Results and Discussion

4.1 Quantum chemical calculation

According to the litterature the two habitually orbitals that are involved in chemical stability are the LUMO (lowest unoccupied molecular orbital) and the HOMO (highest occupied molecular orbital). The LUMO represents the capacity to gain an electron while the HOMO represents the capacity to yield an it. The LUMO and HOMO energies have been calculated thanks to the B3LYP/6-31G(d) method.[38] The transition from the ground state to the first excited one represents the electronic absorption. Such a transition is described by an electronic excitation from the HOMO to the LUMO in the optimized structures of the two compounds (**Fig. 4**).

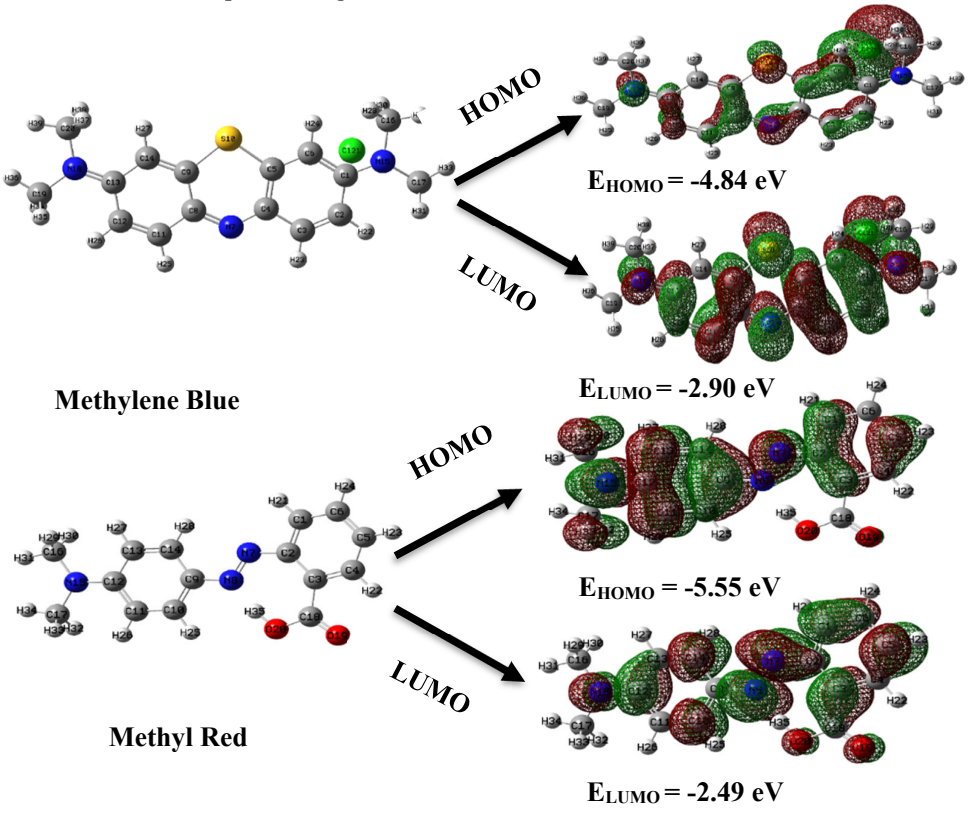

Fig. 4. HOMO and LUO of methylene blue and methylene red.

The extracted energies of HOMO, LUMO, and the energy gap ΔE of MB and MR molecules are presented in **Table 1**. Hence, lower absolute value of ΔE = (E_{HOMO}-E_{LUMO}) gaps correspond to better chemical reactivity of the compound. This gap is considered as the main factor controlling the physicochemical properties of π-conjugated systems. In fact, the mobility of the π electrons means that large aromatic systems have, like MB and MR, promotes good conductivity as in the case of semiconductors having a lower conduction band gap. In fact, the movement of electrons, in the studied compounds, could generate an electrical current.[39]

The following quantum descriptors have been calculated from the two obtained optimized structures.

Ionization potential: $IP = -E_{HOMO}$ (1)

Electronic affinity: $EA = -E_{LUMO}$ (2)

Absolute electronegativity: $$x = \frac{IP + EA}{2}$$ (3)

Global hardness: $$\eta = \frac{IP - EA}{2}$$ (4)

Global softness: $$\sigma = \frac{1}{\eta} = -\frac{2}{E_{HOMO} - E_{LUMO}}$$ (5)

Electronic chemical potential: $$\mu = -\frac{(IP + EA)}{2}$$ (6)

Maximum charge transfer: $$\Delta Nmax = -\frac{\mu}{\eta}$$ (7)

Global electrophilicity index: $$\omega = \frac{\mu^2}{2\eta}$$ (8)

Global nucleophilicity index: $N = E_{HOMO} - E_{HOMO\ (TCE)}$ (9)

$E_{HOMO\ (TCE)}$ = -9.37 eV is calculated by DFT/ B3LYP/6-31G(d). The theoretical values of the open circuit voltage V_{OC} have been calculated according to the following expression.

$$V_{OC} = (1/e)\ |E_{HOMO\ (donor)}|-|E_{LUMO\ (acceptor)}|-0.3\ V \quad (10)$$

where the 0.3 Volt term, in equation (10), represents the empirical factor proposed by Scharber and collaborators.[7]

Table 1. Quantum theoretical descriptors of compounds calculated using B3LYP/6-31G(d).

Parameters	E_{HOMO} (eV)	E_{LUMO} (eV)	ΔE (eV)	IP (eV)	EA(eV)	μ (eV)	χ (eV)
MB	-4.84	-2.90	-1.94	4.84	2.90	-3.87	3.87
MR	-5.55	-2.49	-3.06	5.55	2.49	-4.02	4.02

Parameters	η (eV)	σ (eV^{-1})	ω (eV)	N (eV)	ΔN_{max} (eV)	V_{OC} (V)
MB	0.97	1.03	7.73	4.52	3.99	0.84
MR	1.53	0.65	5.28	3.81	2.63	1.55

The ionization potential (IP) is defined as the amount of energy required to remove an electron from a molecule. That is to say that a high ionization energy indicates a high stability hence a chemical inertness. On the other hand, a low ionization energy shows that the molecule tends to be more reactive. Electron affinity (EA) is defined as the energy released when an electron is added to a neuter molecule. That is, a large value (EA) indicates that the molecule tends to retain its electrons. A negative chemical potential (μ) shows that the molecule is stable, i.e., it is difficult for the molecule to break down into its own elements. The hardness (η) of a molecule characterizes the resistance of its electron cloud to deformation when the molecule undergoes small disturbances. A large HOMO-LUMO energy gap indicates that the molecule is hard and exhibits low polarizability and low chemical and biological activities but high kinetic sensitivity, while a small HOMO-LUMO energy gap indicates that the molecule is soft and exhibits high polarizability and chemical and biological activities but low kinetic sensitivity.

According to the **Table 1** the two compounds studied have shown calculated values of the ionization potential (I), the electron affinity (A), the chemical potential (μ), the hardness (η) and the electrophilicity (ω) that are respectively 4.84, 2.90, -3.87, 0.97 and 7.73 eV, in the case of the MB compound. Comparing the calculated values of these five quantum global descriptors (I, A, μ, η and ω) of the MB compound, in the one hand, to those of the MR compound that are respectively 5.55, 2.49, -4.02, 1.53 and 5.28 eV, on the other hand, one can observe that the MR compound is the stable compound and

that the MB is the chemically reactive one. In fact, a large absolute value of HOMO-LUMO gap implies high kinetic stability and low chemical reactivity, because it is energetically unfavorable to extract electrons from a low-lying HOMO, to add them to a high-lying LUMO, and so to form the activated complex of any potential reaction.[40]

In fact, the HOMO-LUMO gap is related to the chemical hardness (η) of a molecule. The MB shows its absolute value of the energy gap (1.94 eV) lower than that of the MR (3.06 eV) and its global softness (σ) higher (1.03 eV^{-1}) than that of the MR (0.65 eV^{-1}). However, the MR electronic chemical potential (-4.02 eV) is slightly lower than the MB one (-3.87 eV). These values may contribute to higher chemical reactivity of the MB compared to the MR case. In fact, lowering the band gap is an interesting approach to improve the absorption of light, which leads to higher currents for the purpose of converting the power of a higher way. The maximum open-circuit voltage (V_{OC}) of the solar cell is related to the energy difference between the highest occupied molecular orbital (E_{HOMO}) of the electron donor and the lowest unoccupied molecular orbital (E_{LUMO}) of the electron acceptor. Electron acceptor, taking into account the energy lost during the generation of photo-charges.[41]

In fact, in the case of organic materials, and by analogy with inorganic semiconductors, the highest occupied molecular orbital (HOMO for Highest Occupied Molecular Orbital) is assimilated with the valence band (BV) and the lowest unoccupied molecular orbital (LUMO for Lowest Unoccupied Molecular Orbital) with the conduction band (BC) (**Fig. 5**). The HOMO is made up of the π bonding electronic levels, while the LUMO is made up of the vacant π* antibonding electronic levels. As it is illustrated by the HOMO and LUMO bands thus established then make it possible to define the oxidation energy of the molecule or ionization potential (Ip), the electron affinity (EA) and the width of the forbidden band or band gap (E_{gap}) as being the energy difference between the allowed bands. The PCBM is an -n-type semiconductor, with energy levels at -3.70 eV for LUMO and -6.10 eV for HOMO. Similarly, methylene blue and methyl red are a p-type semiconductor. Their energy levels are -2.92 eV for LUMO and -4.84 eV for HOMO in the case of methylene blue and -2.49 eV for LUMO and -5.55 eV for HOMO in the methyl red one. So, the value of the open circuit voltage (Voc) can be easily determined from the difference between the two levels: LUMO of donor and HOMO of acceptor.

By following the theoretical value of the V_{oc} of the studied compounds as shown in **Table 1**, one can observe that the voltage of MR (1.55 V) is higher than that of MB (0.84 V). The two compounds that have been studied in the present work are endowed with Voc values comparable to those reported, in the literature [42-44], on organic materials. According to such a result both of the MR and MB compounds may be applied, as conjugated aromatic systems, in photovoltaic organic cells, thanks to the π electrons of the two compounds structures.

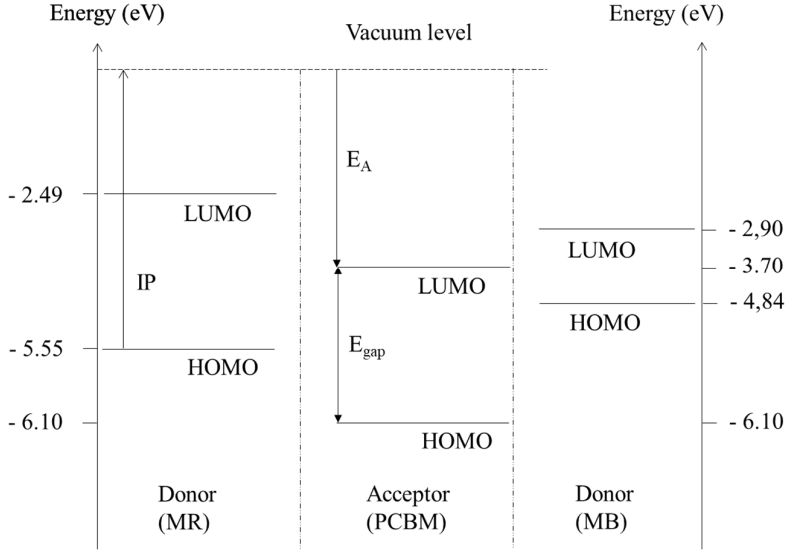

Fig. 5. Donor/acceptor materials energy diagram for the proposed OPV Cell: Donor is methyl red (MR) or methylene blue (MB).

4.2 Non-linear optical properties

Intermolecular interactions in such organic compounds as MB and MR are broadly understood by the dipole moment and the energy terms of first- and second order hyperpolarization. The dipole moment is an important parameter that describes the interaction among atoms. It is the product of the magnitude of charges and the distance between them. The values for the distribution of charges in x, y, and z-directions are listed in **Table 2**.[45] The dipole moment (μ), polarizability

(α), first hyperpolarizability (β), and second hyperpolarizability (γ) have been calculated by the DFT method using the 6-31G(d) base. The equations for calculating the magnitude of μ, α, β and γ, using the x, y, z components of the Gaussian output 09W, are as follows.[46]

$$\mu = (\mu_x^2 + \mu_y^2 + \mu_z^2)^{1/2} \quad (11)$$

$$\alpha = \frac{(\alpha_{xx} + \alpha_{yy} + \alpha_{zz})}{3} \quad (12)$$

$$\beta = (\beta_x^2 + \beta_y^2 + \beta_z^2)^{1/2} \quad (13)$$

with:

$$\beta_x = \beta_{xxx} + \beta_{xyy} + \beta_{xzz}$$
$$\beta_y = \beta_{yyy} + \beta_{xxy} + \beta_{yzz}$$
$$\beta_y = \beta_{yyy} + \beta_{xxy} + \beta_{yzz}$$

$$\beta_z = \beta_{zzz} + \beta_{xxz} + \beta_{yyz}$$

,

$$\gamma = \frac{1}{5}(\gamma_{xxxx} + \gamma_{yyyy} + \gamma_{zzzz} + 2\left[\gamma_{xxyy} + \gamma_{yyzz} + \gamma_{xxzz}\right] \quad (14)$$

The results of descriptors related to the nonlinear optic properties (NLO) of the two compounds are shown in the **Table 2**.

Table 2. Calculated electric dipole moment and first- and second polarizability by method DFT of (A) methylene blue, (B) methyl red using B3LYP/6-31G(d).

	Parameters	MB	MR
Dipole moment (Debye)	μ_x	-8.92	-8.46
	μ_y	-0.93	-5.25
	μ_z	-7.47	0.00
	μ	**11.67**	9.96
Polarizability (Debye)	α_{xx}	-89.10	-79.39
	α_{yy}	-125.89	-120.12
	α_{zz}	-158.62	-118.60
	α	-124.54	-106.04
First Hyperpolarizability (Debye)	β_{xxx}	-237.77	-219.04
	β_{xyy}	-0.89	-61.83
	β_{xzz}	-61.21	0.23
	β_{yyy}	-8.64	-47.46
	β_{xxy}	-24.67	-85.91
	β_{yzz}	0.14	9.59
	β_{zzz}	-35.05	-0.000
	β_{xxz}	-127.20	0.04
	β_{yyz}	-3.97	0.01
	β	**344.47**	306.72
Second Hyperpolarizability (Debye)	γ_{xxxx}	-9315.13	-7999.78
	γ_{yyyy}	-1369.49	-1584.55
	γ_{zzzz}	-812.58	-128.12
	γ_{xxyy}	-1962.02	-1914.52
	γ_{yyzz}	-371.22	-283.95
	γ_{xxzz}	-2425.64	-1742.15
	γ	**-4202.98**	-3518.74

According to **Table 2** the magnitude of the dipole moment of the MB compound is globally relatively higher than that of the MR one. However, the magnitude of the first order hyperpolarizability of the MB compound is globally higher than

that in the case of the MR compound. This is due to intramolecular charge transfer (ICT) between the electron donor and acceptor, which plays a crucial role in the nonlinear behavior of a molecule. The magnitude of the second-order hyperpolarizabily obtained for the MB molecule is also higher than that of the case of the MR compound. These results corroborate with these of HOMO-LUMO gap that have just shown that larger is the last gap lower should be the magnitude of polarisability and hyperpolarisabilies. All these results confirm that the MR compound is more stable than the MB one so that the first compound can better resist any degradation caused by its environment during a possible photovoltaic use.

4.3 Molecular electrostatic potential

The 3D plot of the MEP and contour electrostatic potential for the MB and MR compounds exhibited in **Fig. 6** has been obtained at the DFT/B3LYP/6-31G(d) base. The electrostatic potential at the surface of the two compounds are shown by three different colors. The red color parts indicate the regions that present negative electrostatic potential, the blue sites correspond to the regions that present positive electrostatic potential and the parts marked in green color represent the zones of zero potential. The MEP map shows the negative potential sites on chlorine as well as the positive potential sites around the hydrogen atoms.[47] For the two compounds the values of the local electrostatic charges at the level of the atoms have a magnitude that does not exceed almost the 9.10^{-2} C order. One can easily observe, in the **Fig. 6** at left, that the red color large zone represents the negative parts around the chlorine of MB compound (electrophiles active zones), the blue color represents the positive parts (the nucleophilic zones) and the green color represent the zones with zero electrostatic potential. In the **Fig. 6** at right, the red zone corresponds to the environment of the oxygen atoms in the MR compound.

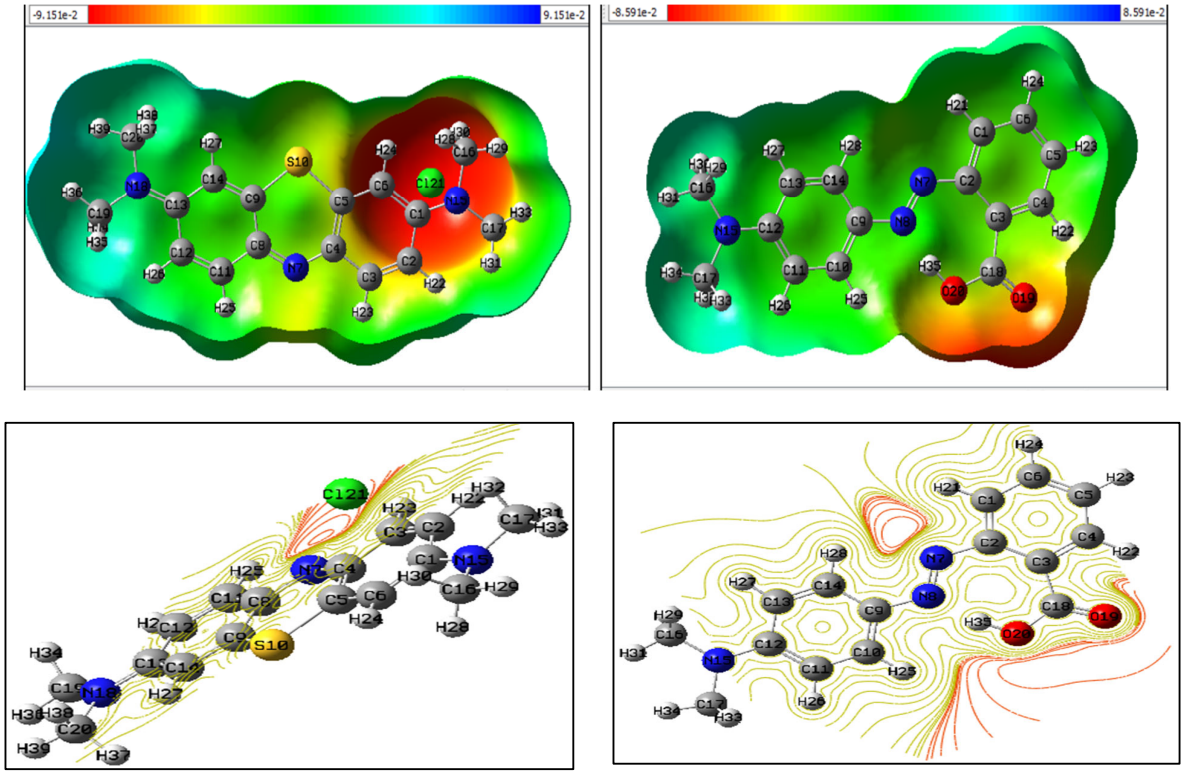

(A) (B)

Fig. 6. Electrostatic potential maps and contour electrostatic potential around the molecule of (A) methylene blue, (B) methyl red.

4.4. UV-visible spectra of the methylene blue and methylene red

This work has been carried out by the TD DFT B3LYP/6-31G(p) method, absorption, and emission properties of the two optimized molecular structures. Effectively, we have calculated the UV-Vis spectrum of the studied MB and MR compounds using TD-DFT method. As illustrated in **Table 3**, we can observe that the values of calculated wavelength λmax, oscillator strength (f), in the case of excitation to the S1 state, correspond almost exclusively to the promotion of an

electron from the HOMO to the LUMO orbital. The electronic transitions**,** excitation energies, wavelength, and oscillator strengths for the three excited states of the MB and MR molecules are presented in the **Table 3**:

Table 3. Data absorption spectra obtained by TD/DFT method ON the MB and MR molecules studied in the optimized geometries at B3LYP/6-31G(d).

Transition state	Molecule	E_{ex} (eV)	λ (nm)	OS (eV)
First	MB	1.36	909.49	0.00
	MR	2.69	460.99	0.00
Second	MB	1.38	895.39	0.00
	MR	2.98	416.66	0.92
Third	MB	2.09	592.14	0.39
	MR	3.48	356.49	0.00

It is known that the photovoltaic performance of a material crucially depends on its carrier transfer dynamics and that they are closely related to the oscillator strength (OS). Effectively, the larger the oscillator strength of the electronic transition, the larger the carrier transfer in the photovoltaic cell. **Fig. 7** illustrates the predicted UV-Vis spectrum of the MB and the MR compounds. Generally, the absorption wavelengths increase progressively with the increasing of conjugation lengths. It should be prudent to convert a set of calculated transition energies and intensities into an absorption profile. We have compared globally the results of the present work, in terms of calculated maximum wavelengths in the two cases of MB and MR that we carried out on the two compounds to those of experimental works that are quoted in the literature where the each one of these two compounds was in a solvent [48,49]. **Fig. 7** and **Table 3** show that the polarity of the solvent used in two previous experimental studies [48,49] on MB and MR had a bathochromic effect on the two calculated spectra, without solvent, in the present study. In fact, **Fig. 7A** shows that the maximum absorption band of MB, predicted by the solvent-free calculation in the present work, at 592.14 nm was experimentally detected to be around 660 nm. [48] **Fig. 7B** also shows that the maximum absorption band of MR, predicted by the solvent-free calculation in the present work, at 416.66 nm was experimentally detected to be around 540 nm. [48] The oscillator strength corresponding to the MB maximal absorption band is 0.39, whereas it is 0.92 in the case of MR.

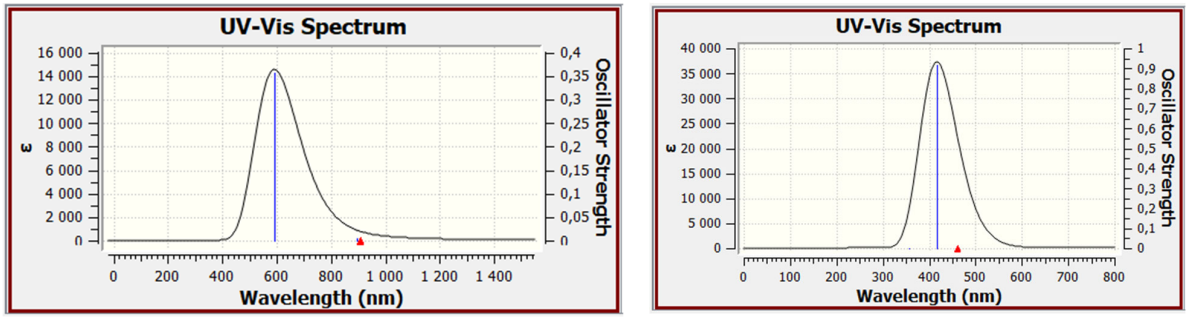

(A) (B)

Fig. 7. UV-Vis spectrum of compounds: (A) methylene blue and (B) methyl red.

This work confirms the high importance of organic molecules in different applications and there are a lot of published papers confirms this point. [50-56]

5. Conclusion

All the obtained calculations in the present work on the methylene blue and methyl red compounds have been carried out at the B3LYP levels and a 6-31G(d) base. We have ensured the optimization of gradient geometry and used both these levels and base that are included in the Gaussian package 09 as depending parameters on the density functional theory (DFT). After having avoided any constraint in the surface potential energy at the Hartree-Fock level, the generated initial geometry from the standard geometric parameters has been optimized. The UV-Vis spectrum has been studied using the time-dependent density functional theory (TD-DFT) method. In order to reach a cost-effective approach for the calculation of the molecular structure, electrostatic potential, Non-linear optical (NLO) and optimized structure energies one can used the theory gradient corrected density function with three hybrid functional parameters (so-called B3) for the exchange part and the Lee-Yang - Parr correlation function (so-called LYP). The first results of the present study have shown an important photovoltaic performance of both methylene blue and methyl red dyes. Thus, we are exploring the carrier transfer dynamics

of the methylene- red and blue molecules by means of measuring, based on Marcus' theory, the rate of charge transfer and charge recombination processes. Through the present work, we have been interested to propose an organic photovoltaic cell of ITO/((MB or MR):PCBM)/Al configuration using results of DFT and TD DFT calculations The one-diode model of the D/A junction has been chosen to characterize performances of the organic solar cell. The developed photovoltaic cell project has used energetic and electrical parameters that can describe the PVO cell based on ([MB or MR]: PCBM). The results of the present work had shown an important circuit voltage, especially in the case of methyl red, more than that case of the methylene blue. The values that are obtained in terms of oscillator strength corresponding to each of the two dyes at the maximum absorption band favor their application in organic photovoltaic cells. These obtained results are in an agreement with the literature results that have been previously published. So, such results of the present work could allow to ensure better performances of the organic photovoltaic cells based on MB and MR molecules. The results of the present work should be confirmed by experimental studies on methylene blue and methyl red compounds in order to be able to ensure their use in solar cells application.

Disclosure statement: *Conflict of Interest:* The authors declare that there are no conflicts of interest.

Compliance with Ethical Standards: This article does not contain any studies involving human or animal subjects.

References

1. Song D., Jiao H., and Te Fan C. (**2015**) Overview of the photovoltaic technology status and perspective in China. *Renew. Sustain. Energy Rev*., 48, 848-856. doi:10.1016/j.rser.2015.04.001
2 Zhang S., and He Y. (**2013**) Analysis on the development and policy of solar PV power in China. *Renew. Sustain. Energy Rev.,* 21, 393-401. doi:10.1016/j.rser.2013.01.002
3 Mulligan C. J., Bilen C., Zhou X., Belcher W. J., and Dastoor P. C. (**2015**) Levelised cost of electricity for organic photovoltaics. *Sol. Energy Mater Sol. Cells,* 133, 26-31. doi:10.1016/j.solmat.2014.10.043
4 Etzold I. A., and Howard R. M. (**2011**) Ultrafast exciton dissociation followed by nongeminate charge recombination in PCDTBT: PCBM photovoltaic blends. *J. Am. Chem. Soc*., 133(24), 9469. doi:10.1021/ja201837e
5 Lee M. R., Eckert R. D., Forberich K., Dennler G., Brabec C. J., and Gaudiana R. A. (**2009**) Solar power wires based on organic photovoltaic materials. *Scie.,* 324(5924), 232-235. doi:10.1126/science.1168539
6 Søndergaard R. R., Hösel M., and Krebs F. C. (**2013**) Roll-to-Roll fabrication of large area functional organic materials. *J. Poly. Scie. Part B: Poly. Physi*., 51(1), 16-34 doi:10.1002/polb.23192
7 Scharber M. C., Mühlbacher D., Koppe M., Denk P., Waldauf C., Heeger A. J., and Brabec C. J. (**2006**) Design rules for donors in bulk-heterojunction solar cells—Towards 10% energy-conversion efficiency. *Adva. mate.,* 18(6), 789-794. doi:10.1002/adma.200501717
8 Capelle K. (**2006**) A bird's-eye view of density-functional theory. *Braz. J. Phys*., 36, 1318-1343. doi:10.1590/s0103-97332006000700035
9 Hotta S., and Lee, S. A. (**1999**) Various chemical modifications of oligothienyls and oligophenyls, *Synth. meta*., 101(1-3), 551-552. doi:10.1016/S0379-6779(98)00845-5
10 Scheidt W. R., and Ellison M. K. (**1999**) The synthetic and structural chemistry of heme derivatives with nitric oxide ligands. *Acco. Chem. resea.,* 32(4), 350-359. doi:10.1021/ar9700116
11 Kalinowski J., Giro G., Cocchi M., Fattori V., and Di Marco P. (**2000**) Unusual disparity in electroluminescence and photoluminescence spectra of vacuum-evaporated films of 1, 1-bis ((di-4-tolylamino) phenyl) cyclohexane. *Appli. Physi. Lett.,* 76(17), 2352-2354. doi:10.1063/1.126343
12 Schwendeman I., Hwang J., Welsh D. M., Tanner D. B., and Reynolds J. R. (**2001**) Combined visible and infrared electrochromism using dual polymer devices. *Advan. Mater.,* 13(9), 634-637. doi:10.1002/1521-4095(200105)13:9<634::AID-ADMA634>3.0.CO;2-3
13 Pei J., Yu, W. L., Huang W., and Heeger A. J. (**2000**) A novel series of efficient thiophene-based light-emitting conjugated polymers and application in polymer light-emitting diodes. *Macromole,* 33(7), 2462-2471. doi:10.1021/ma9914220
14 Yanagi H., and Okamoto S. (**1997**) Orientation-controlled organic electroluminescence of p-sexiphenyl films. Appli. *Physi. Lett.,* 71(18), 2563-2565. doi:10.1063/1.119331
15 Sahdane T., Laghrabli A., Benallal R., Bougharraf H., Azize B., and Kabouchi B. (**2016**) Theoretical Study of The Optical and Photovoltaic Properties of Molecules Based on 1, 3-Diaza-Azulene by DFT Calculations. *J. Chemi. Pharmace. Resea*., 8(9), 130-135.
16 Spaeth C. S., Robison T., Fan J. D., and Bittner G. D. (**2012**) Cellular mechanisms of plasmalemmal sealing and axonal repair by polyethylene glycol and methylene blue. *J. of neuroscie. resea.,* 90(5), 955-966. doi:10.1002/jnr.23022
17. Thompson M. J. (**1984**) Organic Thin Film Transistors for Large Area Electronics. *J Vac Sci Technol B,* 2(4), 827-834. doi:10.1116/1.582902
18 Mozer A.J., and Sariciftci N.S. (**2006**) Conjugated Polymer Photovoltaic Devices and Materials, *C. R. Chim.,* 9 (5-

6), 568-577. doi:10.1016/j.crci.2005.03.033

19 Galagan Y.J., Andriessen R., Rubingh E., Grossiord N., and Blom P. (**2010**) Toward fully printed Organic Photovoltaics: Processing and Stability. *In Proc. LOPE-C*, 88-91.

20. Kasbaji M., Mennani M., Grimi N., Oubenali M., Mbarki M., EL Zakhem H., and Moubarik A. (**2023**) Adsorption of cationic and anionic dyes onto coffee grounds cellulose/sodium alginate double-network hydrogel beads: Isotherm analysis and recyclability performance. *Int J Biol Macromol*., 239,124288. doi:10.1016/j.ijbiomac.2023.124288

21. Kasbaji M, Mennani M, Boussetta A, Grimi N., Barba J. F., Mbarki M., and Moubarik A. (**2023**). Bio-adsorption performances of methylene blue (MB) dye on terrestrial and marine natural fibers: Effect of physicochemical properties, kinetic models and thermodynamic parameters. *Sep Sci Technol*., 58(2), 221-240. doi:10.1080/01496395.2022.2104733

22 Sohrabnezhad S. H. (**2011**) Study of catalytic reduction and photodegradation of methylene blue by heterogeneous catalyst. *Spectrochi. Act. Part A: Molec. Biomolec. Spectro*., 81(1), 228-235. doi:10.1016/j.saa.2011.05.109

23 Fenn A. M., Skendelas J. P., Moussa D. N., Muccigrosso M. M., Popovich P. G., Lifshitz J., and Godbout J. P. (**2015**) Methylene blue attenuates traumatic brain injury-associated neuroinflammation and acute depressive-like behavior in mice. *J. neurotra*., 32(2), 127-138. doi: 10.1089/neu.2014.3514

24. Brokmeier H. M., Troy G., Seelhammer, T. G., Scott D. N., Danielle J. Gerberi D. J., Mara K. C., Erica D. Wittwer E. D., and Wieruszewski P. M. (**2023**) Hydroxocobalamin for Vasodilatory Hypotension in Shock: A Systematic Review With Meta-Analysis for Comparison to Methylene Blue. *J. Cardiothorac. Vasc. Anesth*., 000, 1-16. doi:10.1053/j.jvca.2023.04.006

25. Volke V., Wegener G., Vasar E., and Rosenberg R. (**1999**) Methylene blue inhibits hippocampal nitric oxide synthase activity in vivo. *Brain Res*., 826(2), 303-305. doi:10.1016/S0006-8993(99)01253-6

26 Zhang J. H., Liu Q., Chen Y. M., Liu Z. Q., and Xu C. W. (**2012**) Determination of acid dissociation constant of methyl red by multi-peaks Gaussian fitting method based on UV-visible absorption spectrum. *Act. Physi.-Chim. Sini*., 28(5), 1030-1036. doi:10.3866/PKU.WHXB201203025

27 Jasiński R., Miroslaw B., Demchuk O. M., Babyuk D., and Łapczuk-Krygier A. (**2016**) In the search for experimental and quantumchemical evidence for zwitterionic nature of (2E)-3-[4-(dimethylamino)phenyl]-2-nitroprop2-enenitrile – an extreme example of donor–π–acceptor push–pull molecule. *Journal of Molecular Structure*, 1108, 689-697. doi: 10.1016/j.molstruc.2015.12.056

28 Gadisa A., Svensson M., Andersson M. R., and Inganäs O. (**2004**) Correlation between oxidation potential and open-circuit voltage of composite solar cells based on blends of polythiophenes/fullerene derivative. *Appl. Physi. Lett*., 84(9), 1609-1611. doi:10.1063/1.1650878

29 Becke A. D. (**1992**) Density-functional thermochemistry. I. The effect of the exchange-only gradient correction. *J. Chemi. physi.,* 96(3), 2155-2160. doi:10.1063/1.462066

30 Chen H., Yin Z., Ma Y., Cai D., and Zheng Q. (**2023**) Solution-processed polymer bilayer heterostructures as hole-transport layers for high-performance opaque and semitransparent organic solar cells. *Mater Today Energy*, 35,101322. doi:10.1016/j.mtener.2023.101322

31 Nunzi J.M. (**2002**) Organic Photovoltaic Materials and Devices. *C. R. Phys*., 3, 523-542. doi:10.1016/S1631-0705(02)01335-X

32 Ravi Kishore V. V. N., Aziz A., Narashiman K.L., Periazamy N., Meenakshi P. S., and Wategaonkar S. (**2002**) On the assignment of the absorption bands in the optical spectrum of Alq3. *Synth. Met.,* 126 (2-3),199-205. doi:10.1016/S0379-6779(01)00553-7

33 Theander M., Yartsev A., Zigmantas D., Sundström V., Mammo W., Andersson M.R., and Inganäs O. (**2000**) Photoluminescence quenching at a polythiophene /C_{60} heterojunction. *Phys. Rev. B,* 61, 12957. doi:10.1103/PhysRevB.61.12957

34 Kroeze J. E., Savenije T. J., Vermeulen M. J. W., and Warman J. M. (**2003**) Contactless Determination of the Photoconductivity Action Spectrum, Exciton Diffusion Length, and Charge Separation Efficiency in Polythiophene-Sensitized TiO_2 Bilayers. *J. Phy. Chem. B,* 107, 7696. doi:10.1021/jp0217738

35 Lemaur V., Steel M., Beljonne D., Brèdas J. L., and Cornil J. (**2005**) Photoinduced Charge Generation and Recombination Dynamics in Model Donor/Acceptor Pairs for Organic Solar Cell Applications: A Full Quantum-Chemical Treatment. *J. Am. Chem. Soc.,* 127, 6077-6086. doi:10.1021/ja042390l

36 Şahin G., and Hakkı Alma M. (**2019**) Study of the static characteristic I-V and the electrical parameters corresponding to the shunt resistance Rsh and series resistance Rs per unit area of a solar cell with grain size. *Chinese J Phys.,* 62:395-404. doi:10.1016/j.cjph.2019.09.034

37 Govert den Hartogh (**1995**) The limits of liberal neutrality. *Philosophica,* 56, 59-89.

38 Chattaraj P. K., Duley S., and Domingo L. R. (**2012**) Understanding local electrophilicity/nucleophilicity activation through a single reactivity difference index. *Org. Biomol. Chem.,* 10, 2855-2661. doi: 10.1039/c2ob06943a

39 Scalmani G., Frisch M. J., Mennucci B., Tomasi J., Cammi R., and Barone V. (**2006**) Geometries and properties of excited states in the gas phase and in solution: Theory and application of a time-dependent density functional theory polarizable continuum model. *J. Chem. physi*., 124(9), 094107. doi:10.1063/1.2173258

40 Manolopoulos D. E., May J. C., and Down S. E. (**1991**) Theoretical studies of the fullerenes: C_{37} to C_{70}. *Chem. Phys. Lett*., 181, 105-111. doi:10.1016/0009-2614(91)90340-F

41 Menke S. M., Ran N. A., Bazan G. C., and Friend R. H. (**2018**) Understanding Energy Loss in Organic Solar Cells:

Toward a New Efficiency Regime. *Joule*.*2*, 1-11. doi:10.1016/j.joule.2017.09.020

42 Xiaodong H., Lunxiang Y., and Yanqin L. (**2019**) Design of Organic Small Molecules for Photovoltaic Application. *Journal of Materials Chemistry C,* 7(9), 2487-2521. doi:10.1039/c8tc06589f

43 Raftani M., Abram T., Saidi W., Bejjit L., Bennani N. M., and Bouachrine M. (**2018**) Design of new Organic Materials based on Polythiophene and Polyphenylene for Bulk Heterojunction Solar Cells. THAZES: *Green and Applied Chemistry*, 2(8), 92-102.

44 Bégué D., Guille E., Metz S., Arnaud, M. A., Santos Silva H., Seck M., Fayon P., Dagron-Lartigau C., Iratcabal P., and Hiorns R. C. (**2016**) Graphene-based acceptor molecules for organic photovoltaic cells: A predictive study identifying high modularity and morphological stability. *RSC Adv*., 6, 13653–13656. doi:10.1039/c5ra25531g

45 Proppe A. H., Walters G. W., Alsalloum A. Y., Zhumekenov A. A., Mosconi E., Kelley S. O., Angelis F. D., Adamska L., Umari P., Bakr O. M., and Sargent E. D. (**2020**) Transition Dipole Moments of n = 1, 2, and 3 Perovskite Quantum Wells from the Optical Stark Effect and Many-Body Perturbation Theory. *J Phys Chem Lett*., 11, 716-723. doi:10.1021/acs.jpclett.9b03349

46 El Ouafy H., EL Ouafy T., Oubenali M., EL Haimouti A., Gamouh A., and Mbarki M. (**2021**) Analysis of the Chemical Reactivity of Limonene by the Functional Density Theory Method Using Global Descriptors. *J. Chemi. Heal. Ris.,* 11(2), 213-221. doi:10.22034/jchr.2021.1910282.1189

47 Suramitr S., Kerdcharoen T., Srikhirin T., and Hannongbua S. (**2005**) Electronic properties of alkoxy derivatives of poly(para-phenylenevinylene) , investigated by time-dependent density functional theory calculations. *Synth Met*., 155, 27-34. doi:10.1016/j.synthmet.2005.05.016

48 Lachheb H., Puzenat E., Houas A., Ksibi M., Elaloui E., Guillard C., and Herrmann J. (**2002**) Photocatalytic degradation of various types of dyes (Alizarin S, Crocein Orange G, Methyl Red, Congo Red, Methylene Blue) in water by UV-irradiated titania. *Applied Catalysis B: Environmental*, 39, 75–90. PII: S0926-3373(02)00078-4

49 Tafulo P. A. R, Queirós R. B., and González-Aguilar G. (**2009**) On the "concentration-driven" methylene blue dimerization. *Spectrochimica, Acta*, Part A, 73, 295-300, doi: 10.1016/j.saa.2009.02.033

50 El Tabl A. S., Zawam S., and Shawky Sarhan K. (**2021**) Innovating new methods for wastewater treatment in El-Dakhla Oasis in Upper Egypt from chemical and biological pollutants using modified down Flow Hanging Sponge (DHS) reactor in presence of new environmental friendly chelator. *Egyptian Journal of Chemistry*, 64(9), 4985-4994. doi: 10.21608/EJCHEM.2021.45960.2938

51 Elhady O. M., Mansour E. S., Elwassimy M. M., Zawam S. A., and Drar A. M. (**2022**) Synthesis and characterization of some new tebufenozide analogues and study their toxicological effect against spodoptera littoralis (Boisd.). *Current Chemistry Letters*, 11(1), 63-83. doi: 10.5267/j.ccl.2021.009.005

52 Abdel-Raheem S. A. A., Kamal El-Dean A. M., Abd ul-Malik M. A., Hassanien R., El-Sayed M. E. A., Abd-Ella A. A., Zawam S. A., and Tolba M. S. (**2022**) Synthesis of new distyrylpyridine analogues bearing amide substructure as effective insecticidal agents. *Current Chemistry Letters*, 11(1), 23-28. doi: 10.5267/j.ccl.2021.010.001

53 Elhady O. M., Mansour E. S. , Elwassimy M. M., Zawam S. A., Drar A. M., and Abdel-Raheem S. A. A. (**2022**) Selective synthesis, characterization, and toxicological activity screening of some furan compounds as pesticidal agents. *Current Chemistry Letters*, 11(3), 285-290. doi: 10.5267/j.ccl.2022.3.006

54 Drar A. M., Abdel-Raheem S. A. A., Moustafa A. H., and Hussein B. R. M. (**2023**) Studying the toxicity and structure-activity relationships of some synthesized polyfunctionalized pyrimidine compounds as potential insecticides. *Current Chemistry Letters*, 12(3), 499-508. doi: 10.5267/j.ccl.2023.3.006

55 Ahmed A. A., Mohamed S. K., and Abdel-Raheem S. A. A. (**2022**) Assessment of the technological quality characters and chemical composition for some Egyptian Faba bean germplasm. *Current Chemistry Letters*, 11(4), 359-370. doi: 10.5267/j.ccl.2022.6.001

56 Mohamed S. K., Mague J. T., Akkurt M., Alfayomy A. M., Abou Seri S. M., Abdel-Raheem S. A. A., and Abd Ul-Malik M. A. (**2022**) Crystal structure and Hirshfeld surface analysis of ethyl (3E)-5-(4-chlorophenyl)-3-{[(4-chlorophenyl)formamido]imino}-7-methyl-2H,3H,5H-[1,3]thiazolo[3,2-a]pyrimidine-6-carboxylate. *Acta Crystallographica Section E: Crystallographic Communications*, 78, 846-850. doi: 10.1107/S205698902200603X